

Human Dosimetry of the NMDA Receptor Ligand [^{11}C]GMOM

Jasper van der Aart, Thalia F. van der Doef, Paul Horstman, Marc C. Huisman, Robert C. Schuit, Arthur van Lingen, Albert D. Windhorst, Bart N.M. van Berckel, Adriaan A. Lammertsma

Department of Radiology & Nuclear Medicine, VU University Medical Center,
Amsterdam, The Netherlands

First Author, and contact for correspondence or reprints:

Jasper van der Aart

VU University Medical Center Amsterdam

De Boelelaan 1117, 1081 HV Amsterdam, The Netherlands

Phone: +31610659543

Fax: +31715246499

E-mail: jaspervanderaart@gmail.com

Word count abstract: 147, Word count text: 2472

Figures: 2, Tables: 1

Article Type: Brief Communication

Financial support: This study was supported by the Center for Translational Molecular Medicine (LeARN 02N-101) and European Union's Seventh Framework Programme (FP7/2007-2013), grant agreement n° HEALTH-F2-2011-278850 (INMiND).

Short running title: [^{11}C]GMOM human dosimetry

Abstract

The methylguanidine derivative [^{11}C]GMOM has been used successfully to quantify *N*-methyl-D-aspartate (NMDA) receptor binding in humans. The purpose of the present study was to estimate the [^{11}C]GMOM radiation dose in healthy humans. **Methods:** Following [^{11}C]GMOM injection, three female and two male subjects underwent 10 consecutive whole body PET scans in approximately 77 minutes. 7 source organs were defined manually, scaled to a gender specific reference, and residence times were calculated for input into OLINDA/EXM software. Accepted tissue weighting factors (ICRP103) were used to calculate the effective dose. **Results:** Mean absorbed radiation doses in source organs ranged from 7.7 $\mu\text{Gy}\cdot\text{MBq}^{-1}$ in the brain to 12.7 $\mu\text{Gy}\cdot\text{MBq}^{-1}$ in the spleen. The effective dose ($\pm\text{SD}$) was $4.5 \pm 0.5 \mu\text{Sv}\cdot\text{MBq}^{-1}$. **Conclusion:** The effective dose of [^{11}C]GMOM is at the lower end of the range seen for other C-11 labelled ligands, allowing for serial PET scanning in a single subject.

Key Words: PET; Dosimetry; ^{11}C ; NMDA

Introduction

The phencyclidine (PCP) binding site within the pore of the glutamatergic *N*-methyl-D-aspartate (NMDA) receptor ion-channel is a target for NMDA antagonists such as MK-801 and ketamine. Imaging the PCP site using positron emission tomography (PET) with radiolabelled antagonists has been pursued avidly, but clinical implementation of these radiotracers has been held back by high nonspecific binding, high lipophilicity, low brain entrance, or rapid radioligand metabolism (1). Results from human molecular imaging studies with methylguanidine derivatives such as [^{11}C]CNS 5161 (2) and [^{18}F]GE-179 (3) seem more promising. [^{11}C]GMOM (carbon-11 labelled N-(2-chloro-3-thiomethylphenyl)-N'-(3-methoxyphenyl)-N'-methylguanidine) studies in awake rats showed that administration of the antagonist MK-801 decreased tracer binding in brain regions of interest (ROIs), whereas the channel activator D-serine increased binding (4). Recent experiments in healthy subjects showed that intravenous administration of ketamine $0.3 \text{ mg}\cdot\text{kg}^{-1}$ reduced the [^{11}C]GMOM inhibition constant (K_i) in total brain grey matter by, on average, 66% (5). More human studies with [^{11}C]GMOM are planned, but at present no data on tracer distribution and radiation dose are available. Although various methods can be used to scale dose estimates from preclinical species to man, potentially significant interspecies differences mean that extrapolation from rodent data should be considered with care (6,7). The purpose of the present study was to calculate [^{11}C]GMOM effective dose in men and women for use in future clinical PET protocols.

Materials and Methods

Subjects and scan protocol

The study was approved by the Medical Ethics Review Committee of the VU University Medical Center Amsterdam and all subjects signed an informed consent form prior to inclusion. Five healthy subjects were included, two males and three females, with a mean (\pm standard deviation, SD) weight of $75.4 \pm 7.0 \text{ kg}$, height of $177 \pm 10 \text{ cm}$, and age of $24.9 \pm 2.5 \text{ years}$. Subjects were screened and health status was

confirmed by blood and urine tests (complete blood count, serum chemistry, drug screen), together with a physical examination and medical history. The scanning protocol was identical to that reported previously (8). Subjects were positioned on the bed of a Philips Gemini TF-64 PET/CT scanner (Philips Medical Systems, Cleveland, OH, USA) and a 35 mAs low-dose whole body CT scan was acquired. [^{11}C]GMOM was synthesized according to methods described previously (5). Following intravenous injection of 376 ± 19 MBq [^{11}C]GMOM, a series of 10 whole-body sweeps was performed, taking 40 s per bed position and typically requiring 11 bed positions to cover the body from the top of the head to the upper thigh. Overlap between bed positions was approximately 50% to maintain a constant axial coverage. Total acquisition time was approximately 77 minutes, i.e. 3.8 times the half-life of carbon-11. Five 0.5 mL venous blood samples per subject were taken manually at 10, 27, 44, 60 and 77 minutes post [^{11}C]GMOM injection for measurement of whole blood radioactivity concentrations.

Data Analysis

All PET scans were reconstructed using the standard time-of-flight reconstruction algorithm, including normalization, and corrections for scatter, randoms, attenuation and dead-time (9). Non-decay corrected radioactivity (Bq) in source organs was used to calculate [^{11}C]GMOM residence times. Source organs (ROIs) were defined manually on relevant slices of either CT or PET images depending on optimal visibility of those organs. ROIs included heart, liver, kidneys, spleen, lungs, thyroid and brain. Organ volume (mL) was derived automatically from the ROIs. The lung ROI was edited manually when its location on the respiration-averaged PET scan differed from that on the CT scan. Individual ROIs were projected onto each serially acquired PET frame, manually adjusted in case of patient motion, and [^{11}C]GMOM time–activity curves (TACs) were generated. Radioactivity per organ volume ($\text{Bq}\cdot\text{mL}^{-1}$) was calculated assuming that the distribution of radioactivity within an organ was uniform. TACs were extrapolated from the last whole-body scan to infinity, assuming only physical decay and no further organ clearance. Red marrow activity concentration was assumed to be one third of the whole blood radioactivity concentration(10).

Standardized uptake values (SUV) were calculated by dividing non-decay corrected tissue radioactivity concentration by injected dose per body weight. [^{11}C]GMOM residence times (i.e. normalized cumulated activities) in the seven source organs were obtained through multiplication of the areas under the TACs with each subject's organ mass. Mass was calculated by scaling reference organ weights from a standard male (73.7 kg) or female (56.9 kg) to each subject's body weight using the software package OLINDA/EXM 1.1 (11). Residence times of the manually drawn source organs of each subject were entered into the software to calculate absorbed dose ($\mu\text{Gy}\cdot\text{MBq}^{-1}$) for the target organs, 24 in total. Multiplication of absorbed doses with tissue weighting factors gave the organ effective doses ($\mu\text{Sv}\cdot\text{MBq}^{-1}$). The factors, which represent each organ's relative risk contribution should the whole body be irradiated uniformly, were taken from the International Commission on Radiological Protection (ICRP) publication 103 (12). Total effective dose is the sum of the organ effective doses.

Results

Figure 1 shows coronal slices of the [^{11}C]GMOM distribution in a female subject as a function of time. Figure 2 shows subject-averaged SUVs for the manually delineated ROIs. In early time frames, [^{11}C]GMOM concentrations are highest in lungs, spleen, kidneys and thyroid. Mean residence times are shown in Table 1. The longest residence time (0.0368 ± 0.0093 hours) was observed in the liver, the shortest in the thyroid (0.0005 ± 0.0002 hours). In all subjects, the organ with the highest absorbed dose was the spleen (mean $12.7 \mu\text{Gy}\cdot\text{MBq}^{-1}$). The mean effective dose was $4.5 \pm 0.5 \mu\text{Sv}\cdot\text{MBq}^{-1}$ (males $4.3 \pm 0.8 \mu\text{Sv}\cdot\text{MBq}^{-1}$ and females $4.6 \pm 0.4 \mu\text{Sv}\cdot\text{MBq}^{-1}$).

Discussion

Organ radiation exposure for the NMDA-receptor radiotracer [^{11}C]GMOM was measured in five healthy subjects. The mean effective dose was $4.5 \pm 0.5 \mu\text{Sv}\cdot\text{MBq}^{-1}$. Therefore, a PET scan following an injection of 370 MBq [^{11}C]GMOM would lead, on average, to a radiation dose of 1.67 mSv, which is in the range of

other carbon-11 labelled tracers (7,13). 2222 MBq injected activity would lead to a radiation dose of 10 mSv, which is the limit for proof of concept studies in normal subjects according to ICRP 62 guidelines and The Dutch Commission on Radiation Dosimetry (14). For institutions following organ dose limits for radiopharmaceuticals that are administered under U.S. Radioactive Drug Research Committee regulations, the maximum injected activity per study would be limited by the critical organ rather than the (whole body) effective dose. The critical organ in this study was the spleen with an absorbed dose of $12.7 \mu\text{Gy}\cdot\text{MBq}^{-1}$, which is equivalent to 4.7 mSv for a typical injection of 370 MBq of [^{11}C]GMOM.

Radiotracer dose deposition in tissue depends on both the biological half-life of the compound (and any radiolabelled metabolites) and half-life of the radionuclide. Given the relatively short half-life of carbon-11 (20.4 min), the effective dose mainly depends on organ perfusion and retention. Indeed, in the present study, the highest absorbed doses were found for highly perfused organs. Often, the urinary bladder-wall is reported as being the critical organ, despite delayed filling and the short half-life of carbon-11 (13). [^{11}C]GMOM did not accumulate in the bladder, but rather in the kidneys. This suggests that the main route of tracer excretion is not through the urinary system, and emptying of the bladder will not reduce the dose significantly. The results of the present study are in line with the dosimetry of another methylguanadine derivate, [^{11}C]CNS5161, of which the highest dose was also observed in lungs and spleen (15).

A whole-body scan (from brain to upper thigh) typically required 11 bed positions taking about 7.5 minutes in total. The assumption was made that radiotracer kinetics between first and last bed positions were the same and that the main effect was decay, although this was not the case especially during the early phases of tracer distribution. The resulting uncertainty in organ dose estimates could have been minimized by using shorter PET frames for the first whole-body scans. However, organs with high uptake

in the first frame were located towards the centre of a single bed position (i.e. mid-frame), and overlap between consecutive bed positions was approximately 50% to maintain a constant axial coverage.

Seven organs were designated source organs after visual inspection of the PET images. Absorbed radiation doses in these organs were low (e.g. $12.7 \mu\text{Gy}\cdot\text{MBq}^{-1}$ in spleen) compared with other carbon-11 labelled radiotracers (13). The mean absorbed dose in the critical organ of 32 radiotracers tested in humans was shown to be $40 \mu\text{Gy}\cdot\text{MBq}^{-1}$ (range 11-194), a factor 3 higher than the spleen dose in the present study. Mean ($\pm\text{SD}$) effective dose of the 32 radiotracers was $5.3 \pm 1.5 \mu\text{Sv}\cdot\text{MBq}^{-1}$, half a standard deviation higher than the [^{11}C]GMOM effective dose.

Conclusion

With an effective dose of $4.5 \mu\text{Sv}\cdot\text{MBq}^{-1}$ and relatively low organ doses, [^{11}C]GMOM has a dosimetry profile that allows for serial PET scanning in a single subject.

Disclosure

This study was supported by the Center for Translational Molecular Medicine (LeARN 02N-101) and European Union's Seventh Framework Programme (FP7/2007-2013), grant agreement n° HEALTH-F2-2011-278850 (INMiND). No other potential conflict of interest relevant to this study was reported.

References

1. Fuchigami T, Nakayama M, Yoshida S. Development of PET and SPECT probes for glutamate receptors. *Sci World J*. 2015;2015:1-19.
2. Asselin M, Hammers A, Turton D, Osman S, Koepp M BD. Initial kinetic analyses of the in vivo binding of the putative NMDA receptor ligand [C-11]CNS 5161 in humans. *Neuroimage*. 2004;22:T137.
3. McGinnity CJ, Hammers A, Riaño Barros D a, et al. Initial evaluation of 18F-GE-179, a putative PET Tracer for activated N-methyl D-aspartate receptors. *J Nucl Med*. 2014;55(3):423-430.
4. Waterhouse RN, Slifstein M, Dumont F, et al. In vivo evaluation of [11C]N-(2-chloro-5-thiomethylphenyl)-N'-(3-methoxy-phenyl)-N'-methylguanidine ([11C]GMOM) as a potential PET radiotracer for the PCP/NMDA receptor. *Nucl Med Biol*. 2004;31(7):939-948.
5. van der Doef TF, Golla SS, Klein PJ, et al. Quantification of the novel N-methyl-d-aspartate receptor ligand [11C]GMOM in man. *J Cereb Blood Flow Metab*. 2016;36(6):1111-1121.
6. Sparks, RB; Aydogan B. Comparison of the effectiveness of some common animal data scaling techniques in estimating human radiation dose. In: A. Stelson, M. Stabin, R. Sparks, eds. *Sixth International Radiopharmaceutical Dosimetry Symposium*. Oak Ridge Associated Universities, Oak Ridge, TN, 1999:705–716.
7. Zanotti-Fregonara P, Innis RB. Suggested pathway to assess radiation safety of 11C-labeled PET tracers for first-in-human studies. *Eur J Nucl Med Mol Imaging*. 2012;39(3):544-547.
8. Postnov A, Froklage FE, van Lingen A, et al. Radiation dose of the P-glycoprotein tracer 11C-laniquidar. *J Nucl Med*. 2013;54(12):2101-2103.
9. Surti S, Kuhn A, Werner ME, Perkins AE, Kolthammer J, Karp JS. Performance of Philips Gemini TF PET/CT scanner with special consideration for its time-of-flight imaging capabilities. *J Nucl Med*.

- 2007;48(3):471-480.
10. Sgouros G. Bone marrow dosimetry for radioimmunotherapy: theoretical considerations. *J Nucl Med.* 1993;34(4):689-694.
 11. Stabin MG, Sparks RB, Crowe E. OLINDA/EXM: the second-generation personal computer software for internal dose assessment in nuclear medicine. *J Nucl Med.* 2005;46(6):1023-1027.
 12. International Commission on Radiological Protection (ICRP). ICRP publication 103: the 2007 recommendations of International the International Commission on Radiological Protection. 2007;37:1–333.
 13. Van Der Aart J, Hallett WA, Rabiner EA, et al. Radiation dose estimates for carbon-11-labelled PET tracers. *Nucl Med Biol.* 2012;39(2):305-314.
 14. Publication of the Netherlands Commission on Radiation Dosimetry (Nederlandse Commissie Voor Stralingsdosimetrie NCS). Human Exposure to Ionising Radiation for Clinical and Research Purposes: Radiation Dose & Risk Estimates.
<http://radiationdosimetry.org/documents/ncs/human-exposure-to-ionising-radiation-for-clinical-and-research-purposes-radiation-dose-risk-estimates>. Published 2016. Accessed November 30, 2016.
 15. Dhawan V, Robeson W, Bjelke D, et al. Human Radiation Dosimetry for NMDA Receptor Radioligand 11C-CNS5161. *J Nucl Med.* April 2015:869-872.

Figures and legends

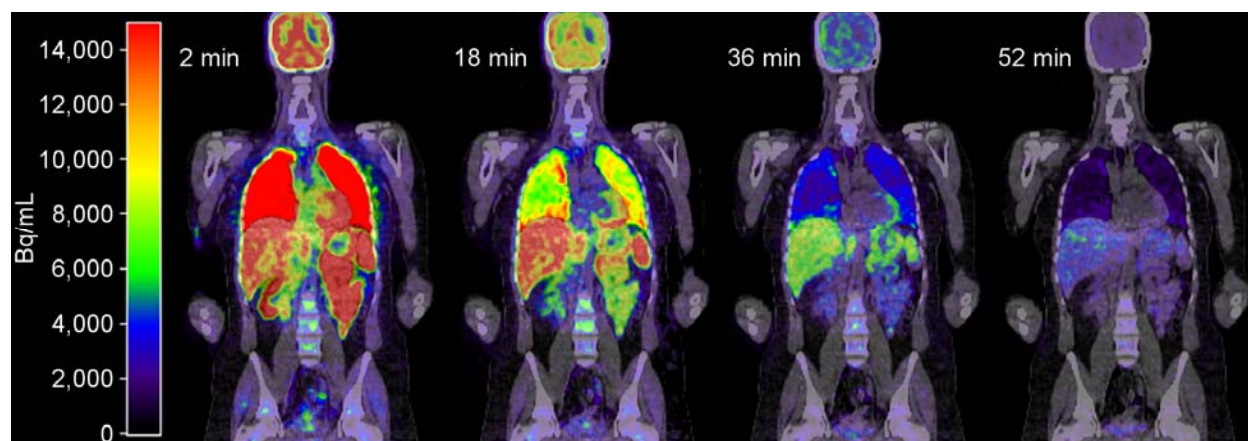


FIGURE 1. Coronal PET/CT fusion images of $[^{11}\text{C}]\text{GMOM}$ uptake in Bq per mL tissue (BQML) showing tracer biodistribution at four different time points (2, 18, 36, and 52 mins) for a female subject. Each panel is a composite of 11 bed positions of 40 seconds each.

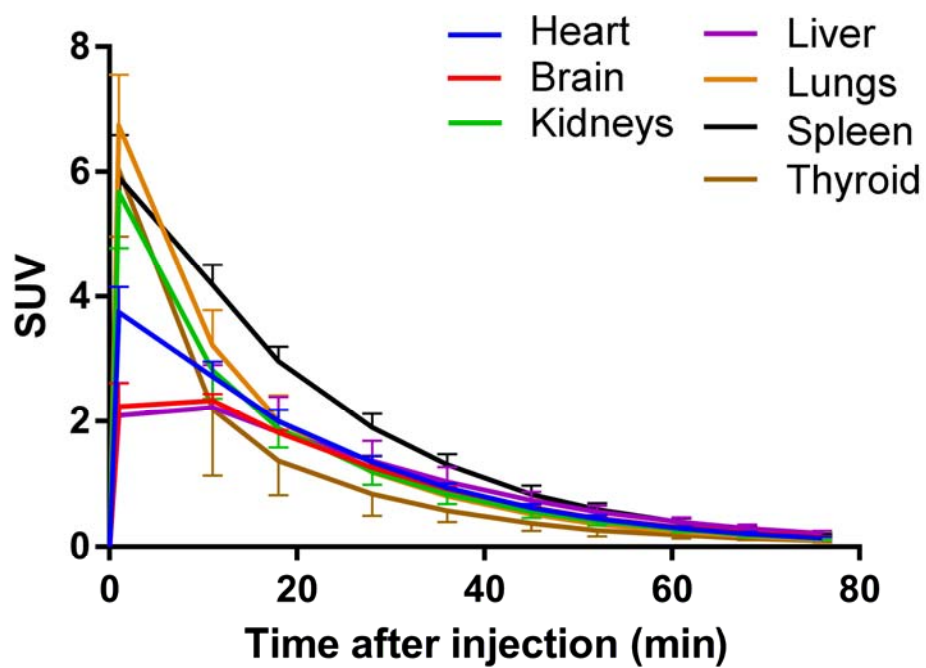


FIGURE 2. Time-standardised uptake value (SUV) curves (non-decay corrected) showing [^{11}C]GMOM SUV (mean and standard deviation of 5 subjects) in manually delineated source organs.

TABLE 1

Organ Doses and Residence Times

Target Organs	Residence Time (Hours)	Absorbed Dose ($\mu\text{Gy}\cdot\text{MBq}^{-1}$)	Effective Dose ($\mu\text{Sv}\cdot\text{MBq}^{-1}$)
Spleen	0.0065 ± 0.0009	12.7 ± 1.5	0.013
Lungs	0.0297 ± 0.0066	10.4 ± 1.9	1.252
Kidneys	0.0086 ± 0.0005	9.8 ± 0.4	0.010
Heart Wall	0.0072 ± 0.0011	9.3 ± 1.3	0.009
Liver	0.0368 ± 0.0093	9.1 ± 2.5	0.362
Thyroid	0.0005 ± 0.0002	8.0 ± 2.3	0.268
Brain	0.0283 ± 0.0033	7.7 ± 1.0	0.077
Pancreas		4.0 ± 0.4	0.004
Adrenals		3.9 ± 0.4	0.004
Gallbladder Wall		3.9 ± 0.4	0.004
Stomach Wall		3.5 ± 0.3	0.421
Total Body		3.5 ± 0.3	0.172
ULI Wall		3.4 ± 0.4	0.409
Ovaries		3.3 ± 0.3	0.261
Thymus		3.3 ± 0.3	0.003
Uterus		3.3 ± 0.3	0.013
LLI Wall		3.2 ± 0.3	0.384
Small Intestine		3.2 ± 0.2	0.003
Muscle		2.9 ± 0.3	0.003
Red Marrow	0.0016 ± 0.0008	2.8 ± 0.2	0.336
Urinary Bladder		2.8 ± 0.2	0.145
Breasts		2.7 ± 0.3	0.326
Skin		2.4 ± 0.2	0.024
Rest		3.5 ± 0.3	0.172
Total Effective Dose			4.5

TABLE 1. Mean \pm SD (n=5) [^{11}C]GMOM residence times (in source organs), absorbed organ doses and effective organ doses. Organs are sorted from highest absorbed dose to lowest. LLI=lower large intestine, ULI=upper large intestine. 'Rest' includes Extrathoracic Region, Oesophagus, Stomach, Lymphatic Nodes and Salivary Glands.